Weak coupling and single-particle structure at high spin in ^{143}Nd

M. Fauerbach, L. A. Riley, P. D. Cottle, R. A. Kaye, and K. W. Kemper
Department of Physics, Florida State University, Tallahassee, Florida 32306
(Received 20 January 1998)

High-spin states of ^{143}Nd have been studied using $\gamma-\gamma$ and γ-conversion electron coincidences. The measurement of 16 new transitions and 8 new conversion coefficients allow revision of the high-spin portion of the level scheme and the determination of parities of six levels for the first time. While the yrast states up to $J=43/2$ can be described using the weak coupling of an $f_{7/2}$ neutron to the ^{142}Nd core nucleus, the new experimental results suggest that weak coupling breaks down above $J=43/2$. This behavior may signal that the closed $N=82$ neutron shell of ^{142}Nd is broken above $J=16$. [S0556-2813(98)05708-2]

PACS number(s): 23.20.Lv, 27.60.+j, 21.60.Cs

High-spin states of spherical nuclei provide an important opportunity to examine the behavior of multiparticle excitations involving high angular momentum orbits. While these configurations can be quite complex, Tekyi-Mensah *et al.* [1] have demonstrated that yrast and near-yrast states in the spherical $N=83$ isotope ^{143}Nd can be understood in a particularly simple way by the weak coupling of an $f_{7/2}$ neutron to the ^{142}Nd core nucleus. The weak coupling model applies over a large range of spins in this nucleus because the yrast states of the core nucleus ^{142}Nd are composed of excitations of the valence protons up to $J=16$ [2]. The single valence neutron of ^{143}Nd does not significantly influence the excited core states and the particle-core coupling remains weak.

In the present work, we address two experimental issues left open by Tekyi-Mensah *et al.* First, many of the states in ^{143}Nd discussed by Tekyi-Mensah *et al.* do not have the parity assignments necessary to confirm the validity of the weak coupling picture. The parity assignments that were presented in Ref. [1] were taken from the results of a singles conversion electron measurement reported by Caussyn *et al.* [3] in which many electron lines of interest were obscured by doublets in ^{143}Nd and other reaction channels. Second, it would be expected that the weak coupling picture would break down when the angular momentum is so high that it is energetically favorable for neutrons to be promoted from the closed $N=82$ shell. This important shift in the structure of ^{143}Nd was not observed by Tekyi-Mensah *et al.*

We present results of $\gamma-\gamma$ and γ-conversion electron coincidence measurements of high-spin states of ^{143}Nd that address both of these issues. First, the γ-electron coincidence condition dramatically improves the quality of electron spectra so that measurements of conversion coefficients that could not be determined with a singles measurement are possible. Second, the thin target required for conversion electron measurements also provides for a smaller yield of a competing reaction channel (^{144}Nd) than in the thick target measurement of Tekyi-Mensah *et al.*, providing more sensitivity for weak γ rays, particularly those deexciting states above $J=20$.

The nucleus ^{143}Nd was produced using the ^{130}Te(^{18}O,5n) reaction with a beam energy of 85 MeV and a target composed of 400 μg/cm^2 of enriched (99.29%) ^{130}Te evaporated onto a 50 μg/cm^2 carbon backing. The ^{18}O beam was produced by the Florida State University Tandem-Superconducting Linear Accelerator Facility. The γ rays were detected with the Florida State University–University of Pittsburgh γ array [4]. Eight Compton-surpressed germanium detectors with a typical resolution of 2.1 keV at 1.33 MeV were used in the present measurement. Conversion electrons were detected with a miniorange spectrometer which included a magnetic filter of the Ishii design [5] and a liquid-nitrogen-cooled Si(Li) detector of 5 mm thickness and 1 cm diameter. The electron spectrometer was placed at 90° to the beam direction. In order to reduce the energy straggling of the electrons inside the target material, the target was positioned at an angle of 45° with respect to the beam axis. The relative efficiencies for the γ-ray detectors and the miniorange spectrometer were determined with an open ^{152}Eu source. Both $\gamma-\gamma$ and γ-electron coincidences were collected.

K-conversion coefficients (α_K) for specific transitions were determined by comparing the yields of electron and γ-ray peaks in spectra gated on the same γ ray. The ratio of these yields was corrected for the relative detection efficiencies and then multiplied by a normalization factor chosen for each set of gated spectra to reproduce a previously measured conversion coefficient. The usefulness of the γ-ray coincidence condition for suppressing the background in the electron measurements is demonstrated in Fig. 1, where the electron and γ-ray spectra gated by the 174 keV γ ray are shown. The K-electron peak for the 247 keV transition,

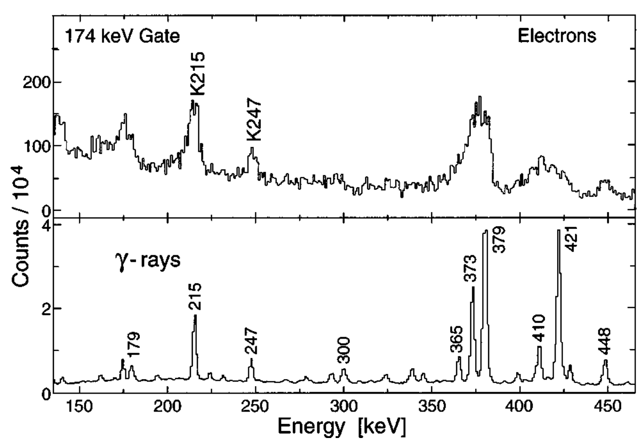

FIG. 1. Electron and γ-ray spectra gated on the 174 keV γ ray. The energy in the electron spectrum includes the K binding energy.

TABLE I. Comparison of K-conversion coefficients and multipolarity assignments as extracted in the present work and in Ref. [3].

E [keV]	α_K This work	α_K Ref. [3]	Multipolarity
140.0	0.30(8)		$E2/M1$
173.8	0.15(4)	0.17(2)	$M1$
179	0.28(11)		
215.0	0.14(2)	0.11(1)	$M1$
223.9	<0.057		$(E1)$
246.7	0.077(19)		$E2/M1$
344.5	0.081(31)		$M1$
364.8	0.035(12)	0.030(4)	$M1$
373.1	0.025(10)	0.025(3)	
379.8	0.036(7)	0.025(3)	$M1$
410.4	0.040(9)	0.034(4)	$M1$
420.9	0.003(7)	0.0047(10)	$E1$
447.7	0.019(5)	0.018(2)	$M1$
485.0	0.018(4)		$E2/M1$
494.6	0.012(3)	0.0083(9)	$E2/M1$
534.1	0.0069(19)	0.0064(10)	
647.2	0.0083(31)		$E2/M1$
709.3	0.010(3)		$E2/M1$
790.9	<0.0015	0.0010(1)	$E1$

which could not be distinguished in the singles conversion electron measurements of Caussyn *et al.* [3], is clearly visible in the gated electron spectrum.

The conversion coefficients determined here are listed in Table I and displayed in Fig. 2, where they are also compared to the results of Caussyn *et al.* [3]. The present results are consistent with those of Ref. [3], and eight new conversion coefficients are determined here as well. In addition, $\gamma-\gamma$ data from this experiment resulted in the observation of 16 new transitions.

In Fig. 3 we show the level scheme for ^{143}Nd as deduced in the present work. The spin assignments for the previously known states were taken from Refs. [1,7]. These assignments

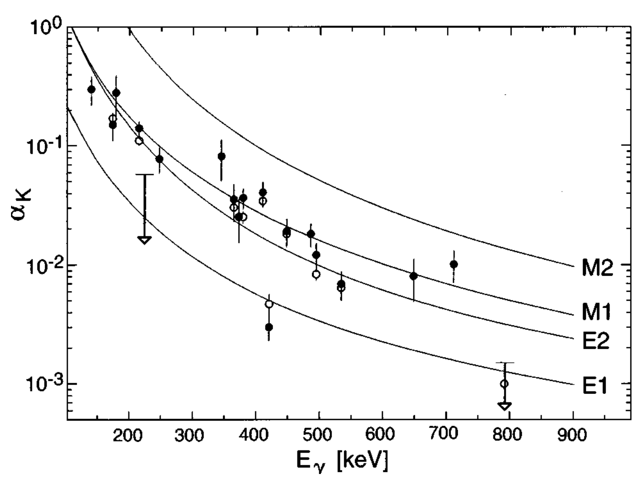

FIG. 2. K-conversion coefficients obtained in the present work (solid circles) and those reported in Ref. [3] (open circles). The theoretical conversion coefficients shown are taken from Ref. [6].

were made either using γ-ray angular distributions [7] or DCO ratios [1]. The present results agree with the previously reported level scheme up to an excitation energy of 8179 keV, except for the ordering of the 379 and 92 keV transitions connecting the level at 2490 keV to the level at 2019 keV. We reverse the order of these transitions because we can clearly observe previously unreported transitions with energies of 1232 and 277 keV in a gate on the 92 keV transition, but not in the spectrum gated on the 379 keV transition. Further support for the ordering proposed here is given by the fact that the 277 keV transition is also seen in a gate on the 456 keV transition populating the level at 3620 keV.

We include one new level (at 3345 keV) and four new transitions in the level scheme below the 8179 keV level. We also observe the three transitions placed in Ref. [1] above 8.2 MeV excitation energy (624, 801, and 1152 keV). However, we add 12 new transitions in this excitation energy range to substantially revise the level scheme. The highest level included here occurs at an excitation energy of 12 MeV. We do not have angular correlation information for transitions above the 8179 keV level, but we say with some confidence that the spins of the states feeding directly to the 8179 keV state (which has $J=43/2$) are either 45/2 or 47/2 because $E1$, $M1$, and $E2$ transitions are those most likely to occur along the yrast line. This includes the three states at 8318, 8717, and 8802 keV. If these three states had spins lower than 45/2, they would likely decay to the 7036 keV 39/2 state because of the large energies these transitions would have.

The new conversion coefficients obtained here allow us to make new parity assignments to six levels. Both the 345 and 711 keV transitions depopulating the 5345 keV level have $M1$, $E2$, or mixed $M1/E2$ multipolarities. Both levels populated by these transitions have positive parity [1], so we can assign positive parity to the 5345 keV state as well. The 215 keV transition depopulating the 5345 keV level is likely to have $M1$ multipolarity, although it may also be $E2$ or mixed $M1/E2$. In any case, this transition connects states of identical parity, so we can assign positive parity to the state populated by the 215 keV transition at 5130 keV. The 5992 keV state is connected to the 5345 keV state by the 647 keV transition, which also has $M1$, $E2$, or mixed $M1/E2$ multipolarity. Therefore, we can assign positive parity to the 5992 keV level as well. The 5992 keV level is connected to the 5507 keV state by the 485 keV transition, which is seen here to have $M1$, $E2$, or mixed multipolarity, yielding positive parity for the 5507 keV level. The 247 keV transition, which is measured to have $M1$, $E2$, or mixed multipolarity, deexcites the 6239 keV level and feeds the 5992 keV level, giving positive parity for the 6239 keV state. We do not have angular correlation data for any of the transitions deexciting the 6239 keV state, so we cannot make a spin assignment. However, this state deexcites to three states having $J=35/2$, so it almost certainly has $J=35/2$, 37/2, or 39/2. Finally, the upper limit we place on the K-conversion coefficient for the 224 keV transition is sufficient to specify an $E1$ multipolarity. This transition depopulates the 5507 keV state and feeds the 5283 keV state, so we can assign negative parity for the latter state.

The multipolarity assignment for the 534 keV transition presents a dilemma. This transition connects the 3024 keV

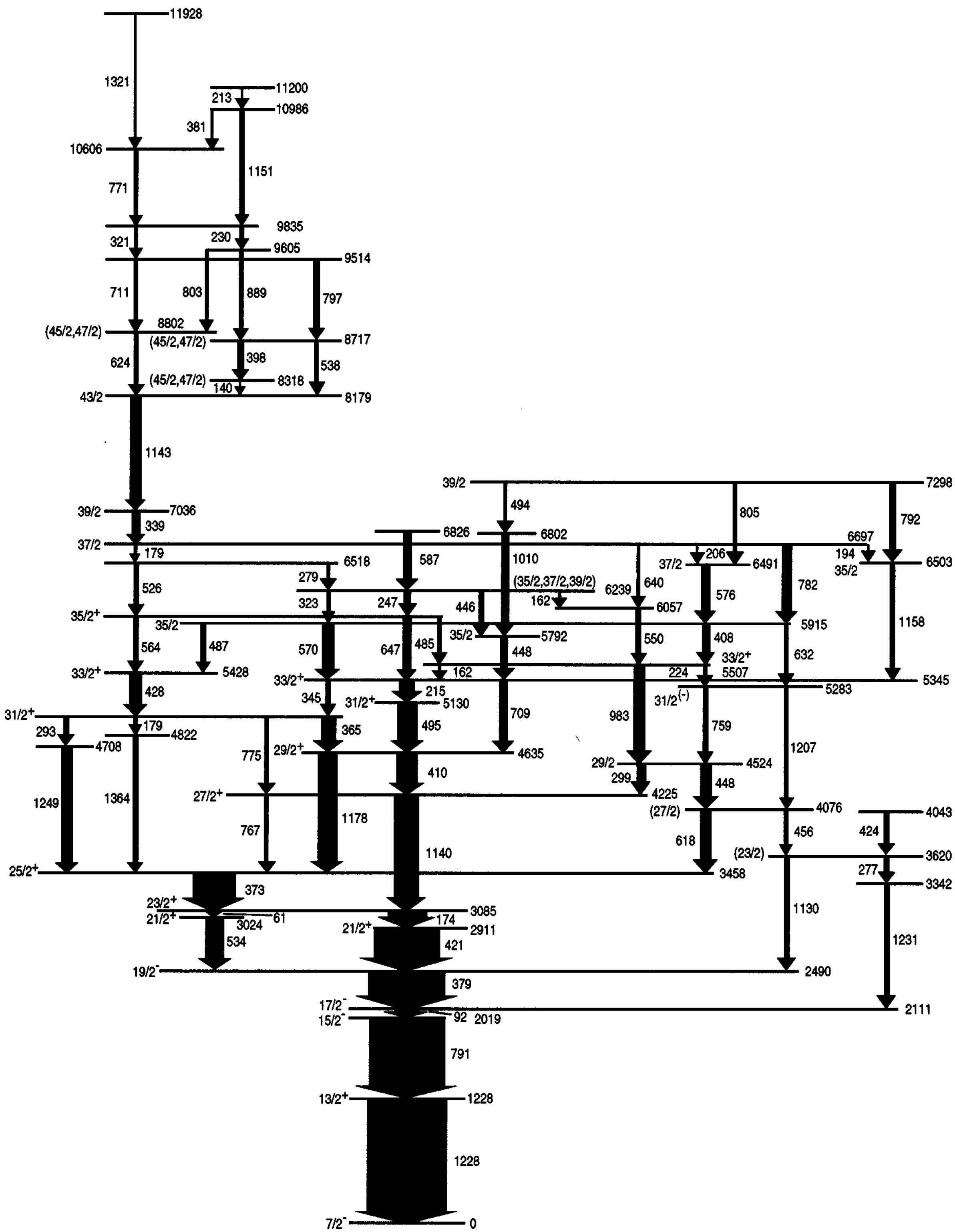

FIG. 3. Level scheme of ^{143}Nd deduced in the present work.

level to the 2490 keV level. The K-conversion coefficient measured here for this transition both agrees with that measured by Caussyn *et al.* [3] and indicates $M1$, $E2$, or mixed multipolarity. However, the 2490 and 3024 keV states appear to have different parities because of the γ-ray intensity pattern. The 2490 keV level is required to have negative parity by the results of conversion electron spectroscopy of transitions below this state [3]. On the other hand, the 61 keV transition connecting the 3024 keV state to the negative parity state at 3085 keV must have $M1$, $E2$, or mixed multipolarity to account for the observed intensity pattern [1]. It seems likely that the 534 keV transition is a multiplet and the large conversion coefficient observed does not reflect the multipolarity of this particular transition.

Although conversion coefficients were extracted for transitions with energies of 179 and 448 keV, we are not able to assign multipolarities to those, as several transitions with very similar energies are known in ^{143}Nd.

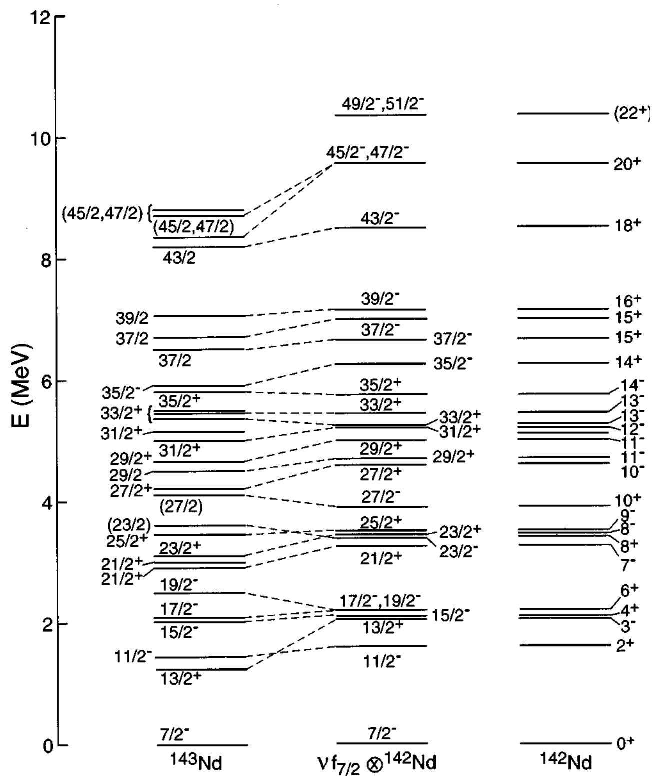

FIG. 4. A comparison of yrast states and several non-yrast states seen in ^{143}Nd with the predictions of a simple weak coupling model. The corresponding states of ^{142}Nd [2] are also shown.

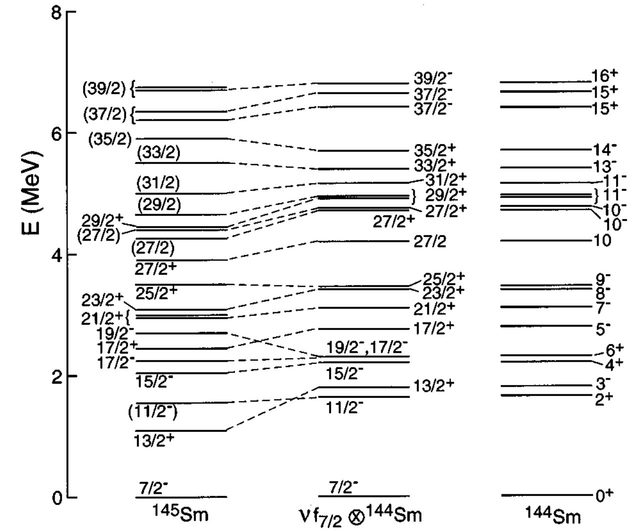

FIG. 5. A comparison of yrast states and several non-yrast states seen in ^{145}Sm [12] with the predictions of a simple weak coupling model. The corresponding states of ^{144}Sm [13] are also shown.

The yrast states of ^{143}Nd shown in Fig. 3 are compared to the simple weak coupling picture ($f_{7/2}$ neutron coupled to ^{142}Nd) in Fig. 4. Several nonyrast states in ^{143}Nd are also included in Fig. 4 because they are easily identified with states in ^{142}Nd. The weak coupling model we discuss here is the simplest possible: it is assumed that no interaction exists between the valence neutron and the states of the ^{142}Nd core. In a detailed analysis of the multiplets arising in ^{143}Nd from the coupling of the $f_{7/2}$ neutron to the 2_1^+, 4_1^+, and 6_1^+ states in the ^{142}Nd core, Wrzesinski *et al.* [8] demonstrated that all members of these multiplets are located at excitation energies within a few hundred keV of the excitation energy of the corresponding ^{142}Nd core states. This result validates the use of our no-interaction model for the present purpose of identifying yrast and near-yrast states in ^{143}Nd with the corresponding core states in ^{142}Nd.

Figure 4 demonstrates that the no-interaction scheme is quite successful up to $J=43/2$ despite its simplicity. The one clear exception to this is the $13/2^+$ state at 1228 keV. However, this state appears to have a more complex structure than the other yrast states: it has a strong—34 Weisskopf units (W.u.)—$E3$ transition to the ground state, indicating it has a large collective octupole component, as well as a large $L=6$ spectroscopic factor (0.45) in the ^{142}Nd(d,p) reaction [9], signalling a large $i_{13/2}$ single neutron component. The mixing of the $i_{13/2}$ neutron state with the state arising from the coupling of the octupole phonon and the $f_{7/2}$ neutron state in the $N=83$ even-Z nuclei was highlighted by Trache *et al.* [10]. While the involvement of the $i_{13/2}$ neutron orbit perturbs energy of the $13/2^+$ state from its weak coupling value, it is likely that the interaction between the $f_{7/2}$ neutron and the octupole phonon is significant as well. The collective octupole vibration in ^{142}Nd—and therefore also in ^{143}Nd—involves a strong contribution from the $N=82$ neutron core. Strong neutron core contributions to the octupole vibration in even-even $N=82$ nuclei have been demonstrated via the comparison of (p,p') and electromagnetic measurements of $B(E3;0^+_{\mathrm{g.s.}}\rightarrow 3^-_1)$ matrix elements in the $N=82$ isotones ^{138}Ba, ^{140}Ce, and ^{144}Sm [11]. Since neutron promotions across the $N=82$ shell gap play a significant role in the octupole vibration, the interaction of the valence $f_{7/2}$ neutron with the core octupole state is likely to be significant so that weak coupling does not apply.

As shown in Fig. 5, a $f_{7/2}$ neutron weak coupling picture can also explain the yrast spectrum of the $N=83$ isotone ^{145}Sm [12] up to $J=39/2$, which corresponds to spin of $J=16$ in the ^{144}Sm core nucleus. In this nucleus, as in ^{143}Nd, the greatest deviation at low and moderate spins occurs for the $13/2^+$ state at 1105 keV, which has a collective octupole component [$B(E3;7/2^-_{\mathrm{g.s.}}\rightarrow 13/2^+_1)=32$ W.u.] and a large $i_{13/2}$ single neutron component [$L=6$ spectroscopic factor of 0.49 in ^{144}Sm(d,p)] [14,10].

The present data on ^{143}Nd also suggest that weak coupling breaks down above $J=43/2$. The lowest $J>18$ state in ^{142}Nd is the 20^+ state at 9532 keV. This is the lowest core state that can generate $J\geqslant 45/2$ states in ^{143}Nd via coupling with an $f_{7/2}$ neutron, so we would not expect $J\geqslant 45/2$ states to occur more than a few hundred keV below 9.5 MeV. However, as explained above, the states at 8318, 8717, and 8802 keV are very likely to have $J=45/2$ or 47/2. As shown in Fig. 4, this deviation is much larger than those for yrast states of lower spins (with the exception of the $13/2^+$ state). This apparent breakdown in the weak coupling picture may indicate a change in the structure of states in the ^{142}Nd core nucleus. Wirowski *et al.* [2] pointed out that spins of up to $J=16$ can be achieved in ^{142}Nd with four quasiproton excitations, but that higher spins must involve more complex structures. It may be energetically favorable in this nucleus to break the $N=82$ neutron core to achieve $J>16$. If this is the case, the neutron excitations will probably interact strongly with the single valence neutron so that the weak coupling picture no longer applies. In the case of ^{143}Nd, it appears that we are using the single valence neutron to probe the microscopic structure of high-spin states of the ^{142}Nd core nucleus.

A comparison of branching ratios for corresponding states in ^{142}Nd and ^{143}Nd could provide an additional test of the weak coupling model. However, information on γ-ray intensities in ^{142}Nd has not yet been published in a form that allows this comparison to be made.

In summary, we have measured 16 new transitions and 8 new electron conversion coefficients near the yrast line in ^{143}Nd and substantially revised the level scheme above 8.2 MeV. The new results support the interpretation of the level scheme up to $J=43/2$ in terms of a simple weak coupling model, but suggest the breakdown of weak coupling above this angular momentum. This may indicate that the closed $N=82$ shell in ^{142}Nd is broken above $J=16$.

This work was supported by the National Science Foundation and the State of Florida.

[1] O.J. Tekyi-Mensah, P.D. Cottle, P.V. Green, J.W. Holcomb, G.D. Johns, J.L. Johnson, T.D. Johnson, K.W. Kemper, P.L. Kerr, S.L. Tabor, P.C. Womble, and V.A. Wood, Phys. Rev. C **50**, R1759 (1994).

[2] R. Wirowski, J. Yan, A. Dewald, A. Gelberg, W. Lieberz, K.P. Schmittgen, A. von der Werth, and P. von Brentano, Z. Phys. A **329**, 509 (1988).

[3] D.D. Caussyn, S.M. Aziz, P.D. Cottle, T. Glasmacher, and K.W. Kemper, Phys. Rev. C **43**, 2098 (1991).

[4] S.L. Tabor, M.A. Riley, J. Döring, P.D. Cottle, R. Books, T. Glasmacher, J.W. Holcomb, J. Hutchins, G.D. Johns, T.D. Johnson, T. Petters, O.J. Yekyi-Mensah, P.C. Womble, L. Wright, and J.X. Saladin, Nucl. Instrum. Methods Phys. Res. B **79**, 821 (1993).

[5] M. Ishii, Nucl. Instrum. Methods **127**, 53 (1975).

[6] F. Rosel, H.M. Fries, and K. Alder, At. Data Nucl. Data Tables **21**, 91 (1978).

[7] S.M. Aziz, P.D. Cottle, K.W. Kemper, M.L. Owens, and S.L. Tabor, Phys. Rev. C **41**, 1268 (1990).

[8] J. Wrzesinski, A. Clauberg, C. Wesselborg, R. Reinhardt, A. Dewald, K.O. Zell, P. von Brentano, and R. Broda, Nucl. Phys. **A515**, 297 (1990).

[9] L.K. Peker, Nucl. Data Sheets **64**, 429 (1991).

[10] L. Trache, A. Clauberg, C. Wesselborg, P. von Brentano, J. Wrzesinski, R. Broda, A. Berinde, and V.E. Iacob, Phys. Rev. C **40**, 1006 (1989).

[11] M.A. Kennedy, P.D. Cottle, and K.W. Kemper, Phys. Rev. C **46**, 1811 (1992).

[12] A. Odahara, Y. Gono, S. Mitarai, T. Morikawa, T. Shizuma, M. Kidera, M. Shibata, T. Kishida, E. Ideguchi, K. Morita, A. Yoshida, H. Kumagai, Y.H. Zhang, A. Ferragut, T. Murakami, M. Oshima, H. Iimura, M. Shibata, S. Hamada, H. Kusakari, M. Sugawara, M. Ogawa, M. Nakajima, B.J. Min, J.C. Kim, S.J. Chae, and H. Sagawa, Nucl. Phys. **A620**, 363 (1997).

[13] J.K. Tuli, Nucl. Data Sheets **56**, 607 (1989).

[14] L.K. Peker, Nucl. Data Sheets **68**, 997 (1993).